

Article

Conceptual Process Design to Produce Bio-Acrylic Acid via Gas Phase Dehydration of Lactic Acid Produced from Carob Pod Extracts

Víctor M. Ortiz Martínez, María I. Saavedra, María J. Salar García *, Carlos Godínez, Luis J. Lozano-Blanco and Sergio Sanchez-Segado *

Department of Chemical and Environmental Engineering, Technical University of Cartagena, C/Dr. Fleming s/n, 30202 Cartagena, Spain

* Correspondence: mariajose.salar@upct.es (M.J.S.G.); sergio.segado@upct.es (S.S.-S.)

Abstract: This work discusses the conceptual process design for the integrated production of bio-based acrylic acid from carob pod aqueous extracts. CHEMCAD was used for the process simulation and cost estimation of the relevant equipment. The process was designed for a capacity of 68 kt of carob pod per year, operating 8000 h annually, and involving extraction, fermentation, catalytic dehydration, and distillation to achieve 99.98%_{w/w} acrylic acid as the main product. The economic assessment for the base case suggests a fixed capital investment of EUR 62.7 MM with an internal rate of return of 15.8%. The results obtained show that carob pod is a promising biomass source for the production of bio-acrylic acid.

Keywords: biorefinery; carob pod; acrylic acid; lactic acid; process design



Citation: Ortiz Martínez, V.M.; Saavedra, M.I.; Salar García, M.J.; Godínez, C.; Lozano-Blanco, L.J.; Sanchez-Segado, S. Conceptual Process Design to Produce Bio-Acrylic Acid via Gas Phase Dehydration of Lactic Acid Produced from Carob Pod Extracts. *Processes* **2023**, *11*, 457. <https://doi.org/10.3390/pr11020457>

Academic Editor: Francesca Blasi

Received: 25 November 2022

Revised: 24 January 2023

Accepted: 30 January 2023

Published: 3 February 2023



Copyright: © 2023 by the authors. Licensee MDPI, Basel, Switzerland. This article is an open access article distributed under the terms and conditions of the Creative Commons Attribution (CC BY) license (<https://creativecommons.org/licenses/by/4.0/>).

1. Introduction

The use of renewable sources with the aim of moving from a fossil-based economy to a more sustainable economy based on biomass is the object of numerous research efforts and policy developments to implement this transition [1–3]. The carob tree (*Ceratonia siliqua* L.) is an evergreen tree typical of the Mediterranean region whose pod can be classified into two parts, the kibble (locust bean), which represents between 80–90%_{w/w} of the pod, and the seeds or kernels (locust kernel gum), which account for 20–10%_{w/w} of the pod. The kibble is mainly used for livestock feeding, while the seeds are used to produce locust bean gum, which in turn is very much appreciated by the food industry. The primary composition of carob kibble consists of 32–42%_{w/w} sucrose, 7–10%_{w/w} glucose, 10–12%_{w/w} fructose, and minor amounts of amino acids, minerals, and phenolic compounds [4]. Despite that, carob kibble has minimal commercial value for farmers, and its chemical composition makes it a cheap carbon and nitrogen source to be used in fermentative processes for the production of bio-based chemicals [5]. Among the different bio-based chemicals that can be produced through fermentation processes, lactic acid (LA) is one of the primary platform chemicals for the green chemistry of the future because it has both carboxylic and hydroxyl groups, providing a high versatility to be used as a precursor of several valuable chemicals such as acrylic acid (AA) [6,7]. AA is a bulk chemical that is used in the manufacture of plastics, coatings, adhesives, elastomers, floor polishes, and paints which are mainly produced by propylene oxidation. Around 6 million tons of AA are produced annually. The global market for AA and its derivatives is expected to increase at an annual rate of 3.5% during the 2020–2025 period; therefore, there is great interest in replacing the petrol-based AA with a bio-based equivalent [8].

Several studies have reported the production of AA from bio-based raw materials. One example is the biological conversion of glycerol into 1,3 propanediol (1,3 PDO) and 3-hydroxy propanoic acid (3HP) in anaerobic conditions followed by the aerobic fermentation

of the mixture to oxidized 1,3 PDO into 3HP. Then, 3HP is catalytically dehydrated to produce AA using TiO_2 at 210 °C [9]. Other works have studied the direct production of 3HP through the fermentation of sugars with genetically modified microorganisms such as *Escherichia coli* and *Saccharomyces cerevisiae* [10,11] for further catalytic dehydration. However, the direct fermentation to produce 3HP is still in the early stage to be industrially implemented. On the other hand, although LA is produced industrially via fermentation at a concentration of around 10%_{w/v}, the catalytic dehydration of its secondary hydroxyl group has proven to be difficult due to its resistance to hydrolysis. Recent efforts have been devoted to the development of heterogeneous catalysts such as potassium modified sodium zeolites, resulting in selectivity and conversion improvements [8,12–14]. This work aims to evaluate the techno-economic assessment of a conceptual biorefinery design to produce AA from carob pod via LA dehydration.

2. Methods

2.1. Process Description

The process scheme was conceptually developed based on our laboratory experiments and a thorough scientific literature review [15]. The conceptual process design was simulated in CHEMCAD7 for a capacity of 68 kt of carob pod per year by analogy with our previous work [16]. The proposed process was assumed to operate 8000 h/year and it is composed of the following sections: (i) carob pod storage, (ii) sugar extraction and solids drying, (iii) fermentation, (iv) LA dehydration, and AA recovery.

2.1.1. Storage, Sugar Extraction, and Solid Drying Section

ST-101 in Figure 1 represents the carob pod storage section in contrast to the 2012 design, which assumed pile storage; in this case, a close system using concrete domes was adopted according to the method proposed by Humbird et al. [17]. Cost estimation for our system was calculated by applying Equation (1).

$$\text{Cost}_{\text{this study}} = \text{Cost}_{\text{Humbird et al.}} \times \left(\frac{\text{Capacity (kg/h)}_{\text{this study}}}{\text{Capacity (kg/h)}_{\text{Humbird et al.}}} \right)^{0.6} \times \left(\frac{\text{CEPCI}_{2021}}{\text{CEPCI}_{2010}} \right) \quad (1)$$

where, $\text{Cost}_{\text{Humbird et al.}}$ [17] was USD 24M, $\text{Capacity}_{\text{this study}} = 8.5 \text{ t/h}$, $\text{Capacity}_{\text{Humbird et al. ref. [17]}} = 94.7 \text{ t/h}$, $\text{CEPCI}_{2021} = 761.5$ and $\text{CEPCI}_{2010} = 550.8$.

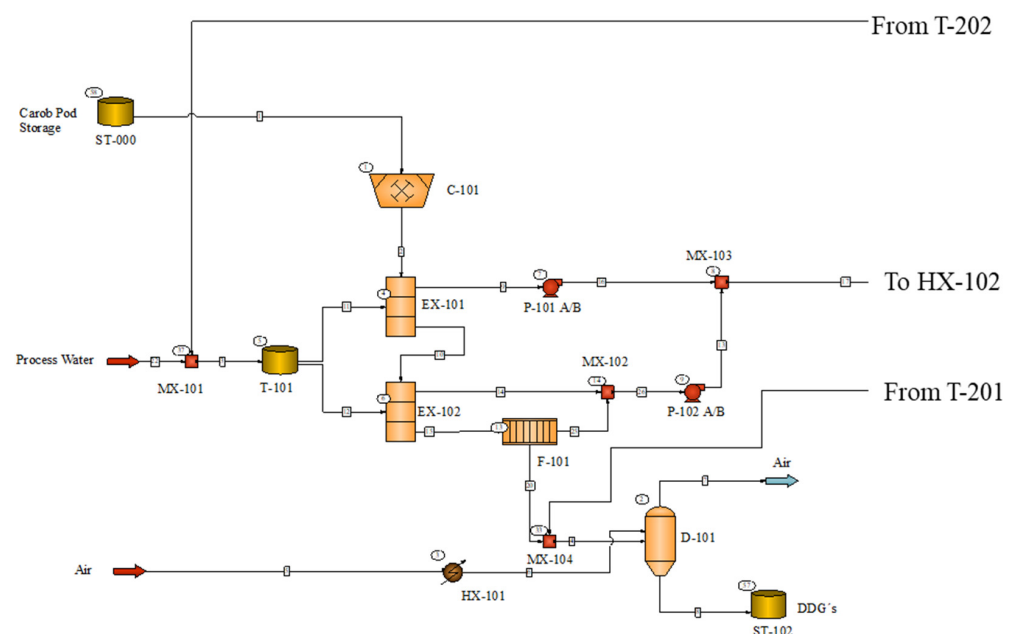


Figure 1. Storage, sugar extraction, and solid drying section process flow diagram.

Carob pulp chemical composition was taken from previous work [4]. The implementation of carob pulp in the CHEMCAD database considers the following assumptions:

1. Moisture percentage was accounted for as H₂O.
2. Since fructose is not present in the CHEMCAD database, its content was added to that of glucose for the sake of simplicity.
3. The quantity of inert material was implemented in CHEMCAD as a pseudo component considering the percentages of protein, fat, fibre, and ash. Its chemical composition was approximated with the data provided by Faik et al. [18] to obtain the empirical chemical formula of C_{4.71}O_{2.81}H_{9.54}N.
4. The thermal properties of the inert material were input into the software following the recommendation given by the American Society of Heating [19]. The chemical composition used in the simulation is listed in Table 1.

Table 1. Carob pulp chemical composition used in the simulation.

Parameter	Value (%w/w)
Moisture	8.4
Glucose	25.0
Sucrose	50.2
Fat *	1.5
Protein *	3.0
Fibre *	8.9
Ash *	3.0

* Fat, fibre, protein, and ash were considered inert materials.

Carob pulp size was decreased from 13 mm to an average size of 0.6 mm in a roller crusher (C-101). After milling, sugars were extracted in two stirred tank reactors (EX-101 and EX-102) with water at room temperature at 700 r.p.m. using an S/L ratio of 0.15 in each reactor to keep a sucrose concentration of 0.11 M at the entrance of R-201. The resulting slurry after sugar extraction was introduced in a filter press to reduce the solid moisture from 62% to 20%. After separation, solids were sent to a rotary dryer (D-101) to obtain a livestock feed with 5% moisture.

2.1.2. Lactic Acid Fermentation Section

The flow diagram of the fermentation section can be seen in Figure 2. The extracted sugars were sterilized in HX-101 by heating the stream up to 98 °C and then cooled down to 34 °C before going into the fermentation section. After sterilization, a fixed bed enzymatic reactor (R-201) was used to hydrolyse sucrose using an invertase load of 95 mg/L. The modelling of this reactor was carried out using the kinetic data provided by the work of Bowski et al. [20]. According to their study, for sucrose concentrations below 0.3 M, the kinetic data can be adjusted to a mixed-order kinetic expression (see Supplementary Information Section S1). Sucrose concentration at the inlet of R-201 is kept at 0.11 M through recirculation of process water from T-202. A continuous fermentation process with *Lactobacillus casei* was considered using a dilution rate of 0.5 h⁻¹ at 37 °C. *L. casei* are Gram-positive, non-sporulating, and strictly fermentative bacteria that produce LA as the main metabolic end product. They can metabolize glucose and fructose but not sucrose. Thus, the assumption of replacing fructose with glucose made in the simulation was expected not to affect the final result [21].

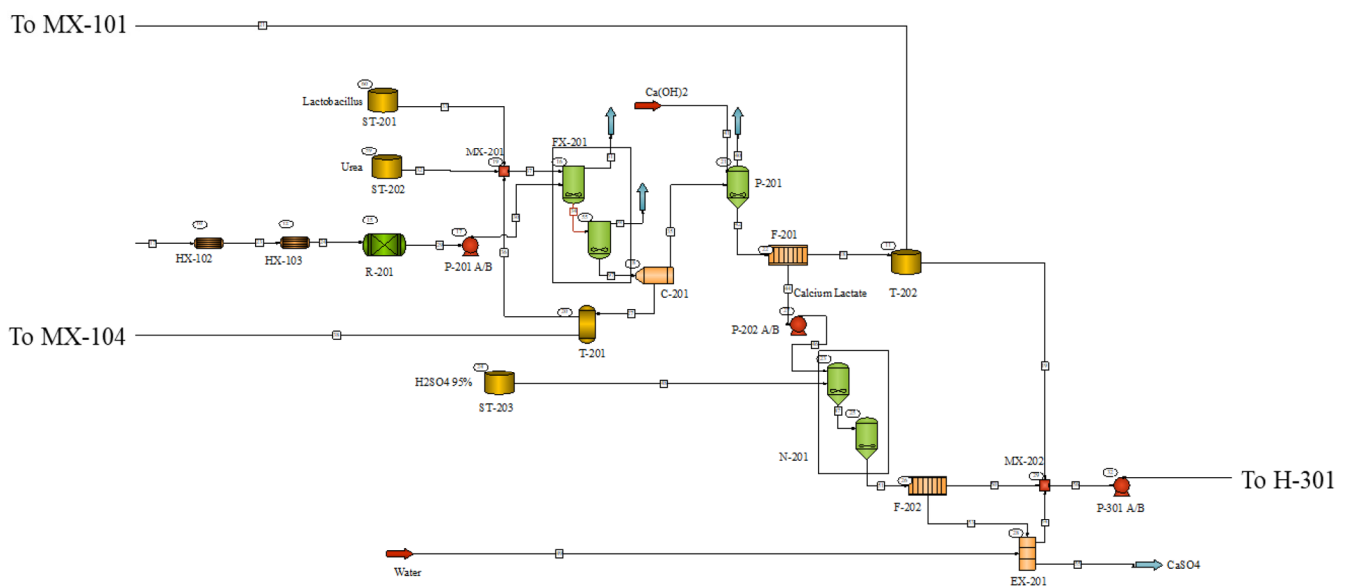
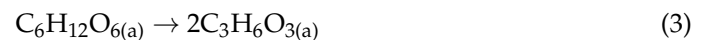
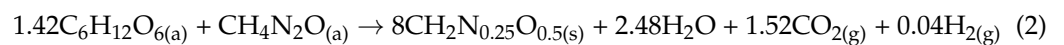
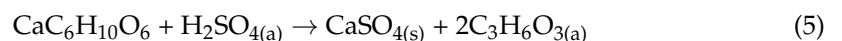
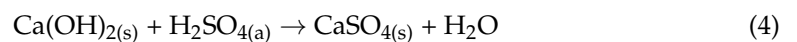


Figure 2. Lactic acid fermentation process flow diagram.

As shown in Figure 2, *L. casei* was transferred from the seed fermentor ST-201 to the production fermenters to provide a 10% inoculum volume. Fermenters were simulated using two stoichiometric reactors (unit FX-201) to take into account the formation of new cells whose empirical formula was considered to be $\text{CH}_2\text{N}_{0.25}\text{O}_{0.5}$ [22]. According to the work by Turhan et al. [23], a total glucose conversion of 97% was implemented (43% accounted for cell growth and 54% for the conversion into LA). Reactions (2) and (3) were used for the stoichiometric reactors:



At the end of the fermentation process, cells were separated by centrifugation in C-201 and mixed with the filtered solid. The fermentation broth was sent to P-201 and mixed with $\text{Ca}(\text{OH})_2$ to precipitate calcium lactate $\text{CaC}_6\text{H}_{10}\text{O}_6$, which was separated from the solution in F-201. A total of 93% of the liquid outlet of F-201 was recycled back to the sugar extraction section and the remaining 7% was used to adjust the concentration of lactic below 50% before its dehydration. $\text{CaC}_6\text{H}_{10}\text{O}_6$ was sent to unit N-201 where it was treated with sulfuric acid to allow for the recovery of LA and neutralize the excess of $\text{Ca}(\text{OH})_2$ following Reactions (4) and (5):

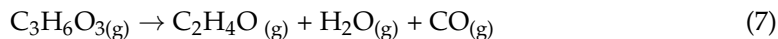
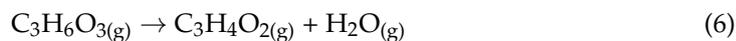


The CaSO_4 formed after acid treatment was washed in unit EX-201 before disposal.

2.1.3. Lactic Acid Dehydration and Acrylic Acid Recovery Section

The process flow diagram of the AA production and the purification section can be seen in Figure 3. The liquid outlet of unit F-202 was mixed with the wash waters of EX-201 and T-202 to keep the LA concentration below 50%_{w/w}. This stream was vaporized and heated in H-301 up to 200 °C. The vaporized stream was introduced in the fixed bed catalytic reactor R-301 where the dehydration of LA took place using potassium ion-exchanged ZMS5 zeolite at 360 °C with a 97% LA conversion [13]. Reactions (6) and (7) were considered for the reactor model, using the kinetic Expressions (8) and (9), which were

obtained from the work reported by Yan et al. [13] and modified to express the reaction rate as a function of the catalyst volume.



$$r_{\text{AA}} = 5.48 \times 10^{16} \times e^{\left(\frac{-152.7}{RT}\right)} \times C_{\text{LA}}^{0.19} \times C_{\text{H}_2\text{O}}^{0.36} \quad (8)$$

$$r_{\text{AD}} = 1.75 \times 10^{16} \times e^{\left(\frac{-165.3}{RT}\right)} \times C_{\text{LA}}^{0.54} \times C_{\text{H}_2\text{O}} \quad (9)$$

where r_{AA} and r_{AD} are the formation reaction rates of AA and acetaldehyde, respectively, in $\frac{\text{mol}}{\text{h m}^3_{\text{cat}}}$, C_{LA} and $C_{\text{H}_2\text{O}}$ are the concentrations of LA and water, respectively, in $\frac{\text{mol}}{\text{m}^3}$, and the activation energies are expressed in $\frac{\text{kJ}}{\text{mol}}$.

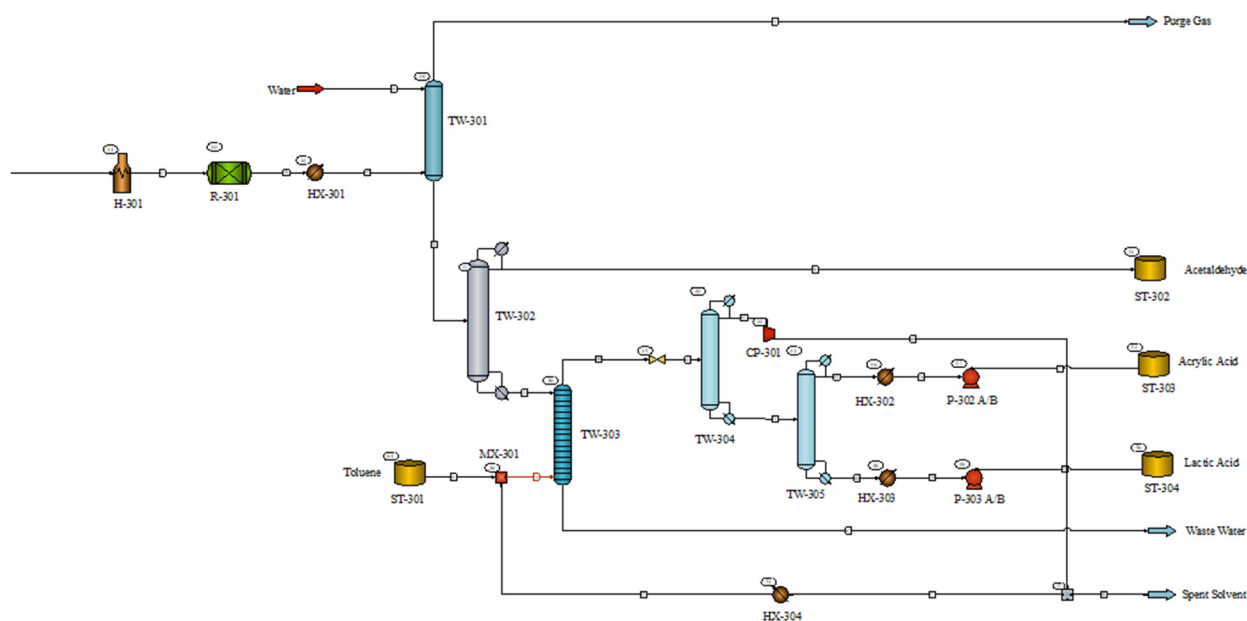


Figure 3. Acrylic acid production and purification process flow diagram.

To avoid AA polymerization, the reactor outlet was cooled down to 50 °C in HX-301, which was used at the same time to generate low-pressure steam at 150 °C. The cooled stream entered the absorption tower TW-301 to remove the light components. Deionized water was used in TW-301 to minimize AA and acetaldehyde losses. The liquid outlet of TW-301 was introduced into the distillation column TW-302 to obtain a distillate rich in acetaldehyde with a 96.06%_{w/w} purity. The liquid outlet of TW-302 was introduced into the liquid–liquid extraction column TW-303, which used toluene as an extraction agent following the recommendations given by Song et al. [24]. After liquid–liquid extraction, the extracted phase moved to a separation train, which consisted of two distillation columns (TW-304 and TW-305) to separate each component with the required commercial assay. Columns TW-304 and TW-305 worked under vacuum (0.16 atm) to keep the system temperature below 90 °C to avoid AA polymerization. The bottoms of column TW-304 rich in AA and LA moved to column TW-305 to obtain a distillate with 99.98%_{w/w} AA and a bottom product with 99.40%_{w/w} LA. The TW-304 distillate containing toluene and water traces was pressurized to 1 atm and recycled to the TW-302 extraction column.

2.2. Economic Evaluation

The CHEMCAD costing tool and the CAPCOST excel spreadsheet developed by Turton et al. [25] were used to determine the installation costs of the majority of the equipment in the process flowsheet. The equipment purchased costs were adjusted to the

desired capacity and relevant time of study using the Chemical Engineering Plant Cost Index (CEPCI) of 761.5 for the year 2021. A summary of the installation equipment cost and the main specifications of each piece of equipment can be found in the supplementary information Table S2. The project life was fixed at 15 years with annual inflation of 6%, following the modified accelerated cost recovery system method.

The total capital investment (TCI) of the plant is the total cost of major equipment, auxiliary equipment, cost of buildings, and other costs, such as contract fees, freight, engineering, contingencies, research, and development. The components of the TCI were estimated using the estimation factors presented in Table S3 [26,27]. For the TCI breakdown, it was considered that the Spanish Council [28] can provide 26% of the TCI (9% of the TCI as a non-refundable grant and 18% of the TCI as a loan to be reimbursed equally for 5 years with an interest rate of 1.69% starting one year after plant operation). Tables 2 and 3 summarize the main economic parameters considered in the evaluation.

Table 2. Economic parameters used in this study.

Parameter	Value
Annual operating hours	8000 h
Project life	15 years
Income tax rate	25%
Inflation rate	6%
Salvage value	4% of the TCI
Carob pod consumption	8500 kg/h
AA production	2416 kg/h
LA production	49 kg/h
AC production	245 kg/h
Animal feed production	3802 kg/h
Construction period	
%Spend in year −2	8%
%Spend in year −1	60%
%Spend in year 0	32%
Start-up time	2 years

Table 3. Manufacturing costs breakdown.

Manufacturing Costs	Value	Unit	Reference
Variable costs			
(a) Feedstock			
Carob pod	0.17	EUR/kg	[29]
(b) Auxiliary raw materials			
H ₂ SO ₄ (98%)	0.23	EUR/kg	
Urea	0.12	EUR/kg	
Ca(OH) ₂	0.19	EUR/kg	
MgSO ₄	0.12	EUR/kg	[30]
MnSO ₄	0.42	EUR/kg	
K ₂ HPO ₄	0.50	EUR/kg	
Sodium Acetate	0.50	EUR/kg	
Process water	3.80×10^{-4}	EUR/kg	
Toluene	0.05	EUR/kg	[31]
Lactobacillus	47.20	EUR/kg	

Table 3. *Cont.*

Manufacturing Costs	Value	Unit	Reference
Compress Air	5.20×10^{-3}	EUR/kg	Own estimation
Invertase	33.00	EUR/kg	Own estimation
Catalysts	1.07	EUR/kg	Own estimation
(c) Utilities			
Cooling water	4.24	EUR/GJ	
Steam	12.71	EUR/GJ	[24]
Natural gas	6.44	EUR/GJ	
Electricity	0.14	EUR/kWh	[31]
(d) Waste Disposal			
CaSO ₄ disposal	0.05	EUR/kg	
Wastewater	3.80×10^{-5}	EUR/kg	[32]
Toluene disposal	0.035	EUR/kg	
(e) Labor			
Direct labor cost	36,500	EUR/employee year	Own estimation
Indirect labor cost	32% of direct labor cost	EUR/year	[16]
(f) Maintenance			
	2% of FCI	EUR/year	
Fixed costs			
Loans and interest	2.10×10^6	EUR/year	[28]
Administrative expenses	3.2% of TCI	EUR/year	[16]
General expenses	3.0% of sales	EUR/year	
Depreciation	Straight line method applied to 63% of TCI over 5 years	EUR/year	Own estimation

Manufacturing Costs

Manufacturing costs have been classified into two categories:

- Variable costs, which include the cost of feedstock, auxiliary raw materials, direct and indirect labor, maintenance, waste disposal, and utilities.
- Fixed costs, which include loans, interest, depreciation, and general and administrative expenses.

For the economic assessment of the base case, the net present value (NPV) was calculated using Equation (10).

$$NPV = -TCI + \frac{\sum_{n=1}^{15} F_n}{(1+i)^n} + \frac{S}{(1+i)^{14}} + \frac{WC}{(1+i)^{14}} \quad (10)$$

where F_n is the annual net cash flow, n is the number of years considered in the project, i is the annual inflation rate, S is the salvage value, and WC is the working capital. The internal rate of return (IRR) was used to estimate the profitability potential of the proposed process. IRR is a discount rate that makes the net present value (NPV) of all cash flows equal to zero in a discounted cash flow analysis. According to Short et al. [33], an IRR value after tax of 10% was selected as the minimum value to consider the process profitable. A sensitivity analysis was performed to study the influence of several parameters, such as operating hours/year, and the price of feedstock, AA, combined utility costs, and auxiliary raw materials on plant profitability. The remaining cost parameters were kept constant.

3. Results and Discussion

3.1. Mass and Energy Balances

The overall mass and energy balance results performed in CHEMCAD are provided in Table 4. Closure on the mass balance was 99.8%; small errors can be attributed to the imperfect stoichiometry used to generate microbial cell mass in fermentation. A total of 91%_{w/w} of the CO₂ emissions were of biogenic origin generated in the fermenters; meanwhile, the remaining CO₂ and CO emissions were produced by the pyrolysis of the unconverted glucose and sucrose. Table 5 shows the composition of the main input and output streams. As can be observed, 2416 kg/h of 99.98%_{w/w} AA could be achieved from 8500 kg/h of carob pod.

Table 4. Overall mass and energy balance.

Overall Mass Balance		
Component	Input (kg/h)	Output (kg/h)
Water	11,737.2	13,405.4
Saccharose	4267	1.7
Glucose	2125	1.2
Inert material	1394.0	1394.0
Air	7233.3	7233.3
Urea	650.0	0.0
Hydrogen	0.0	5.9
Carbon dioxide	0.0	779.1
Lactic acid	0.0	167.3
Lactobacillus	1.0	2211.4
Calcium hydroxide	1565.0	0.0
Sulfuric acid	2071.8	0.2
Calcium sulfate	0.0	2875.6
Acrylic acid	0.0	2526.2
Acetaldehyde	0.0	236.8
Carbon monoxide	0.0	150.4
Toluene	847.0	858.8
Total	31,891.3	31,851.6
Overall Energy Balance		
	Input (MJ/h)	Output (MJ/h)
Feed streams	−305,701	0
Product streams		−343,470
Total heating	86,920	0
Total cooling	−126,643	0
Power added	1316	0
Power generated	0	0

Table 5. Main input–output stream compositions.

Stream	Carob Pod	DDGs	CaSO ₄ Waste	Acetaldehyde	Acrylic Acid	Lactic Acid	Wastewater
Temperature (°C)	25.0	30.0	25.0	42.0	42.0	25.0	67.3
Pressure	1.0	1.0	0.8	1.7	1.0	1.0	1.0
Total mass flow rate (kg/h)	8500.0	3802.3	2875.6	245.1	2416.0	49.4	13,163.3
Component mass flow rate (kg/h)							
Water	714.0	190.11	0.0	7.6	0.0	0.0	12,918.9
Saccharose	4267.0	1.74	0.0	0.0	0.0	0.0	0.0
Glucose	2125.0	1.19	0.0	0.0	0.0	0.0	0.0
Inert material	1394.0	1394.0	0.0	0.0	0.0	0.0	0.0
Air	0.0	0.0	0.0	0.0	0.0	0.0	0.0
Urea	0.0	0.0	0.0	0.0	0.0	0.0	0.0
Hydrogen	0.0	0.0	0.0	0.0	0.0	0.0	0.0
Carbon dioxide	0.0	0.0	0.0	1.6	0.0	0.0	0.0
Lactic acid	0.0	3.72	0.0	0.0	0.7	49.1	114.1
Lactobacillus	0.0	2211.4	0.0	0.0	0.0	0.0	0.0
Calcium hydroxide	0.0	0.0	0.0	0.0	0.0	0.0	0.0
Sulfuric acid	0.0	0.0	0.0	0.0	0.0	0.1	0.1
Calcium sulfate	0.0	0.0	2875.6	0.0	0.0	0.0	0.0
Acrylic acid	0.0	0.0	0.0	0.2	2415.3	0.2	111.8
Acetaldehyde	0.0	0.0	0.0	235.45	0.0	0.0	0.24
Carbon monoxide	0.0	0.0	0.0	0.1	0.0	0.0	0.0
Toluene	0.0	0.0	0.0	0.0	0.0	0.0	18.2

As can be seen in Table 4, the major energy requirements of the process were due to the usage of utilities for heating and cooling streams, accounting for nearly 43% of the total energy input.

3.2. Sensitivity Analysis

3.2.1. Effect of Each Independent Variable

Figure 4a–d show the effect of changing each variable independently over the base case. The effect of operating hours per year in Figure 4a was studied to take into account the seasonal availability of the biomass and/or potential interruptions in the supply. The operating hours/year were changed from 3600 h/year to 8000 h/year. A minimum of 5172 h/year are required to achieve an IRR of 10%. Figure 4b shows the variation of the internal rate of return with the feedstock price. IRR values higher than 10% can be reached for prices below 0.24 EUR/kg. Regarding the acrylic selling price and utility costs, Figure 4c,d show that a minimum selling price of 1.84 EUR/kg and a maximum utility cost of 0.64 EUR/kg make the process profitable.

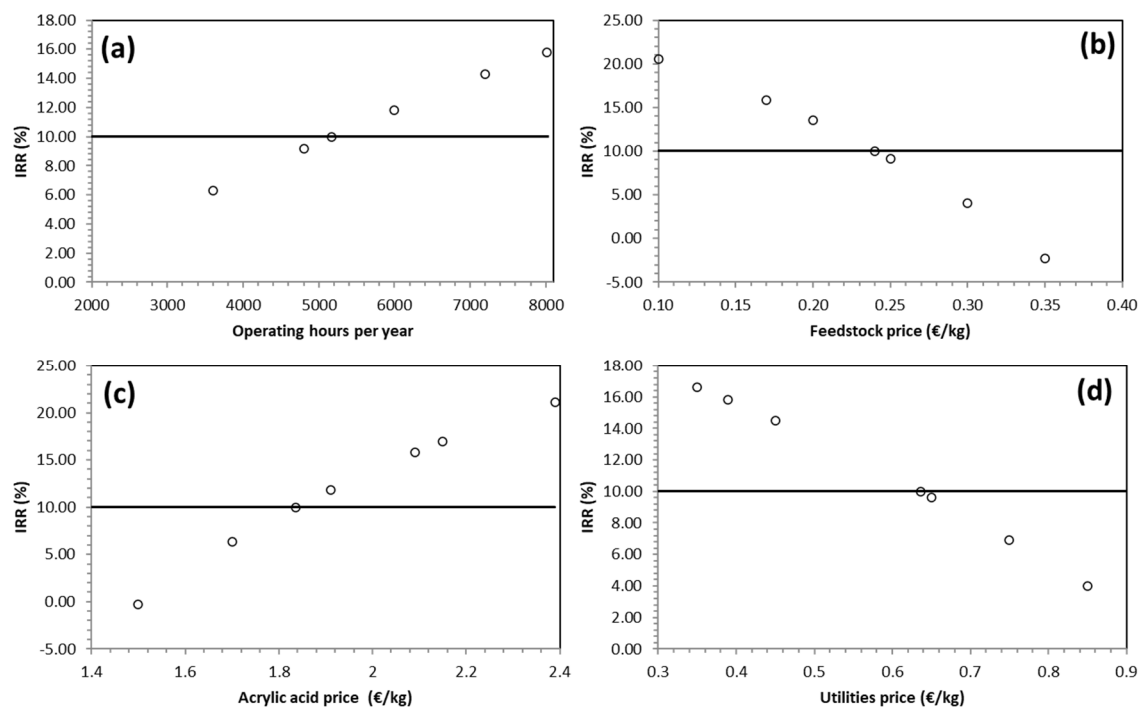


Figure 4. Variation in the internal rate of return with (a) the yearly operating hours, (b) feedstock price, (c) acrylic acid selling price, and (d) cost of utilities.

3.2.2. Effect of Combined Variables

A non-linear multivariable regression analysis was also carried out to study the combined effect of each variable on the IRR. The results achieved are shown in Table 6. In this analysis, both p -value and f -value were employed as statistical parameters for analysing the significance of the variables with a 95% confidence interval ($p < 0.05$).

Table 6. Factorial design of experiments. A: operating hours; B: feedstock price; C: acrylic acid selling price; D: utility cost; and IRR (%): calculated IRR value.

Run	A (h)	B (EUR/kg)	C (EUR/kg)	D (EUR/kg)	IRR (%)
1	5250	0.20	2.20	0.35	10.84
2	2500	0.10	1.90	0.57	2.03
3	5250	0.10	2.20	0.57	12.89
4	5250	0.20	1.60	0.35	-1.14
5	2500	0.20	2.20	0.57	1.56
6	8000	0.20	2.20	0.57	11.55
7	5250	0.10	1.90	0.35	11.90
8	5250	0.20	1.90	0.57	0.82
9	2500	0.20	1.90	0.35	0.61
10	5250	0.20	1.90	0.57	0.82
11	5250	0.20	2.20	0.80	2.52
12	2500	0.10	2.20	0.35	7.06
13	8000	0.20	1.90	0.80	-7.01
14	2500	0.20	1.90	0.57	-2.22
15	8000	0.10	1.90	0.57	13.11

Table 6. Cont.

Run	A (h)	B (EUR/kg)	C (EUR/kg)	D (EUR/kg)	IRR (%)
16	8000	0.10	2.20	0.35	23.08
17	5250	0.30	2.20	0.57	−0.44
18	2500	0.20	1.90	0.80	−6.85
19	5250	0.30	1.90	0.35	−2.59
20	5250	0.10	1.90	0.80	3.66
21	8000	0.20	1.90	0.35	9.90
22	5250	0.20	1.90	0.57	0.82
23	5250	0.10	1.60	0.57	2.05
24	8000	0.10	2.20	0.80	14.53

Figure 5 shows the Pareto chart that depicts the standardized effects with $p = 0.05$. The bar length belongs to the absolute standardized value. As can be seen, all the factors exceed the reference line (2.16), indicating that all of them are statistically significant.

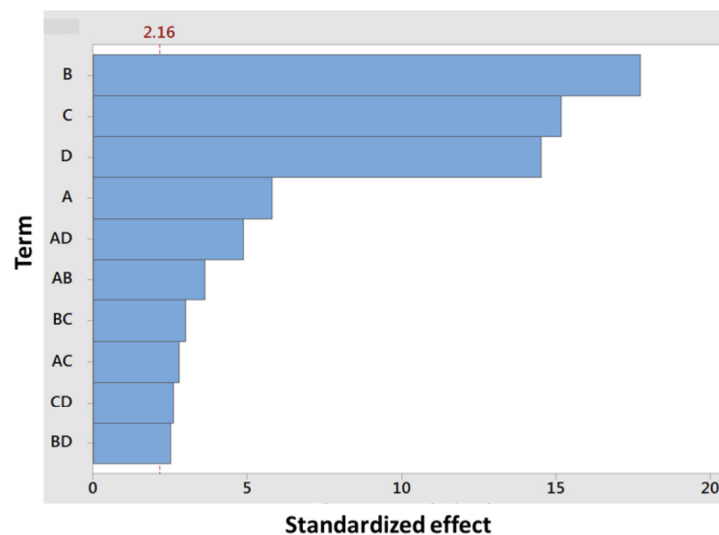


Figure 5. Pareto chart of standardized effects.

The analysis of the variance allows for obtaining the following model equation:

$$\text{IRR} = 22.70 + 3.90 \times 10^{-4} \times A - 115.10 \times B - 12.40 \times C - 35.20 \times D - 8.53 \times 10^{-3} \times A \times B - 2.17 \times 10^{-3} \times A \times C + 3.33 \times 10^{-3} \times A \times D + 59.8 \times B \times C - 61.10 \times B \times D + 21.27 \times C \times D \quad (11)$$

The IRR function evaluated with the Restrictions (12) to (15) shows a maximum IRR value of 16.91 for $A = 8000$ h, $B = 0.15$ EUR/kg, $C = 2.20$ EUR/kg, and $D = 0.50$ EUR/kg:

$$4000 \geq A \leq 8000 \quad (12)$$

$$0.15 \geq B \leq 0.30 \quad (13)$$

$$1.80 \geq C \leq 2.20 \quad (14)$$

$$0.50 \geq D \leq 0.90 \quad (15)$$

4. Conclusions

- Based on the simulation results, the material and energy balances show that the process requires 8.5 t/h of carob pod to produce 2.42 t/h of acrylic acid with an overall energy consumption of 88.9 MJ/kg, which is comparable to the value of 53.2 MJ/kg reported by Bhagwat et al. [8].
- The economic evaluation performed for the base case suggested that a plant operating 8000 h/year with a treatment capacity of 8.5 t/h of carob pulp requires an FCI of EUR 62.7 MM with an IRR

value of 15.8%. The effects of changing the operating hours, acrylic acid selling price, feedstock, and utility costs on the economic performance of the plant were evaluated independently to determine the ranges in which the IRR of the base case is higher than 10%.

- It was concluded that the investment involved a minimum of 5172 h/year of operation, an acrylic acid selling price higher than 1.84 EUR/kg, and carob pulp and utilities costs below 0.24 EUR/kg and 0.64 EUR/kg, respectively.
- A factorial design of the experiments was carried out to evaluate the combined effect of the economic variables selected on the IRR. The analysis of the standardized effect shows that the order of the most significant variables is carob pulp cost > acrylic acid selling price > utility cost > operating hours. Using the analysis of the variance, a model equation showing the relationship of the IRR with the economic variables selected was obtained. The maximum of this function provides an (IRR)_{max} of 16.91% for 8000 h of yearly operation, a feedstock price of 0.15 EUR/kg, an acrylic acid selling price of 2.20 EUR/kg, and a utility cost of 0.50 EUR/kg.

Supplementary Materials: The following supporting information can be downloaded at: <https://www.mdpi.com/article/10.3390/pr11020457/s1>, Figure S1: Kinetic model fitting to experimental data. Table S1: Rate of sucrose hydrolysis by invertase. Table S2: Equipment specification for bio-acrylic acid production from carob pod process at a capacity of 68 kton carob pod per year. Table S3: Factors applied for the calculation of the TCI.

Author Contributions: Conceptualization, S.S.-S.; methodology, V.M.O.M. and M.I.S.; software, S.S.-S.; validation, M.J.S.G. and C.G.; formal analysis, V.M.O.M. and L.J.L.-B.; resources, S.S.-S.; data curation, M.I.S.; writing—original draft preparation, M.I.S. and V.M.O.M.; writing—review and editing, L.J.L.-B. and C.G.; visualization, M.J.S.G. and C.G.; supervision, S.S.-S. and M.J.S.G.; project administration, S.S.-S.; funding acquisition, S.S.-S. and L.J.L.-B. All authors have read and agreed to the published version of the manuscript.

Funding: Sergio Sánchez-Segado and this research were supported by the Spanish Ministry of Education and Vocational Training, grant number “Beatriz Galindo” BEAGAL18/00079.

Data Availability Statement: The data presented in this study are available upon request from the corresponding author.

Conflicts of Interest: The authors declare no conflict of interest.

References

1. Bröring, S.; Laibach, N.; Wustmans, M. Innovation Types in the Bioeconomy. *J. Clean. Prod.* **2020**, *266*, 121939. [[CrossRef](#)]
2. Sanz-Hernández, A.; Esteban, E.; Garrido, P. Transition to a Bioeconomy: Perspectives from Social Sciences. *J. Clean. Prod.* **2019**, *224*, 107–119. [[CrossRef](#)]
3. Stegmann, P.; Londo, M.; Junginger, M. The Circular Bioeconomy: Its Elements and Role in European Bioeconomy Clusters. *Resour. Conserv. Recycl. X* **2020**, *6*, 100029. [[CrossRef](#)]
4. Mahtout, R.; Ortiz-Martínez, V.; Salar-García, M.; Gracia, I.; Hernández-Fernández, F.; Pérez de los Ríos, A.; Zaidia, F.; Sanchez-Segado, S.; Lozano-Blanco, L. Algerian Carob Tree Products: A Comprehensive Valorization Analysis and Future Prospects. *Sustainability* **2018**, *10*, 90. [[CrossRef](#)]
5. Yatmaz, E.; Turhan, I. Carob as a Carbon Source for Fermentation Technology. *Biocatal. Agric. Biotechnol.* **2018**, *16*, 200–208. [[CrossRef](#)]
6. Becker, J.; Lange, A.; Fabarius, J.; Wittmann, C. Top Value Platform Chemicals: Bio-Based Production of Organic Acids. *Curr. Opin. Biotechnol.* **2015**, *36*, 168–175. [[CrossRef](#)]
7. Dusselier, M.; Van Wouwe, P.; Dewaele, A.; Makshina, E.; Sels, B.F. Lactic Acid as a Platform Chemical in the Biobased Economy: The Role of Chemocatalysis. *Energy Environ. Sci.* **2013**, *6*, 1415. [[CrossRef](#)]
8. Bhagwat, S.S.; Li, Y.; Cortés-Peña, Y.R.; Brace, E.C.; Martin, T.A.; Zhao, H.; Guest, J.S. Sustainable Production of Acrylic Acid via 3-Hydroxypropionic Acid from Lignocellulosic Biomass. *ACS Sustain. Chem. Eng.* **2021**, *9*, 16659–16669. [[CrossRef](#)]
9. Dishisha, T.; Pyo, S.-H.; Hatti-Kaul, R. Bio-Based 3-Hydroxypropionic- and Acrylic Acid Production from Biodiesel Glycerol via Integrated Microbial and Chemical Catalysis. *Microb. Cell. Fact.* **2015**, *14*, 200. [[CrossRef](#)] [[PubMed](#)]
10. Kildegaard, K.R.; Wang, Z.; Chen, Y.; Nielsen, J.; Borodina, I. Production of 3-Hydroxypropionic Acid from Glucose and Xylose by Metabolically Engineered *Saccharomyces Cerevisiae*. *Metab. Eng. Commun.* **2015**, *2*, 132–136. [[CrossRef](#)]
11. Cheng, Z.; Jiang, J.; Wu, H.; Li, Z.; Ye, Q. Enhanced Production of 3-Hydroxypropionic Acid from Glucose via Malonyl-CoA Pathway by Engineered *Escherichia Coli*. *Bioresour. Technol.* **2016**, *200*, 897–904. [[CrossRef](#)]
12. Bonnotte, T.; Paul, S.; Araque, M.; Wojcieszak, R.; Dumeignil, F.; Katryniok, B. Dehydration of Lactic Acid: The State of The Art. *ChemBioEng Rev.* **2018**, *5*, 34–56. [[CrossRef](#)]

13. Yan, B.; Liu, Z.-H.; Liang, Y.; Xu, B.-Q. Acrylic Acid Production by Gas-Phase Dehydration of Lactic Acid over K⁺-Exchanged ZSM-5: Reaction Variable Effects, Kinetics, and New Evidence for Cooperative Acid–Base Bifunctional Catalysis. *Ind. Eng. Chem. Res.* **2020**, *59*, 17417–17428. [[CrossRef](#)]
14. Sobuś, N.; Czekaj, I. Lactic Acid Conversion into Acrylic Acid and Other Products over Natural and Synthetic Zeolite Catalysts: Theoretical and Experimental Studies. *Catal. Today* **2022**, *387*, 172–185. [[CrossRef](#)]
15. Sánchez, S.; Lozano, L.J.; Godínez, C.; Juan, D.; Pérez, A.; Hernández, F.J. Carob Pod as a Feedstock for the Production of Bioethanol in Mediterranean Areas. *Appl. Energy* **2010**, *87*, 3417–3424. [[CrossRef](#)]
16. Sánchez-Segado, S.; Lozano, L.J.; de los Ríos, A.P.; Hernández-Fernández, F.J.; Godínez, C.; Juan, D. Process Design and Economic Analysis of a Hypothetical Bioethanol Production Plant Using Carob Pod as Feedstock. *Bioresour. Technol.* **2012**, *104*, 324–328. [[CrossRef](#)] [[PubMed](#)]
17. Humbird, D.; Davis, R.; Tao, L.; Kinchin, C.; Hsu, D.; Aden, A.; Schoen, P.; Lukas, J.; Olthof, B.; Worley, M.; et al. *Process Design and Economics for Biochemical Conversion of Lignocellulosic Biomass to Ethanol: Dilute-Acid Pretreatment and Enzymatic Hydrolysis of Corn Stover*; National Renewable Energy Laboratory: Golden, CO, USA, 2011.
18. Ayaz, F.A.; Torun, H.; Glew, R.H.; Bak, Z.D.; Chuang, L.T.; Presley, J.M.; Andrews, R. Nutrient Content of Carob Pod (*Ceratonia siliqua* L.) Flour Prepared Commercially and Domestically. *Plant Foods Hum. Nutr.* **2009**, *64*, 286–292. [[CrossRef](#)]
19. American Society of Heating, Refrigerating; Air-Conditioning Engineers, Inc. Thermal Properties of Foods. In *2006 ASHRAE Handbook: Refrigeration*; ASHRAE: Atlanta, GA, USA, 2006; ISBN 9781601197948.
20. Bowski, L.; Saini, R.; Ryu, D.Y.; Vieth, W.R. Kinetic Modeling of the Hydrolysis of Sucrose by Invertase. *Biotechnol. Bioeng.* **1971**, *13*, 641–656. [[CrossRef](#)] [[PubMed](#)]
21. Pot, B.; Felis, G.E.; De Bruyne, K.; Tsakalidou, E.; Papadimitriou, K.; Leisner, J.; Vandamme, P. The Genus *Lactobacillus*. In *Lactic Acid Bacteria*; John Wiley & Sons, Ltd.: Chichester, UK, 2014; pp. 249–353.
22. Shuler, M.L.; Fikret, K. *Bioprocess Engineering: Basic Concepts*, 2nd ed.; Prentice Hall: Upper Saddle River, NJ, USA, 2002.
23. Turhan, I.; Bialka, K.L.; Demirci, A.; Karhan, M. Enhanced Lactic Acid Production from Carob Extract by *Lactobacillus Casei* Using Invertase Pretreatment. *Food Biotechnol.* **2010**, *24*, 364–374. [[CrossRef](#)]
24. Song, D.; Yang, J.-H.; Lee, C.-J. Conceptual Design of Water Separation Process in Glycerol-Based Acrylic Acid Production. *Chem. Eng. Res. Des.* **2020**, *156*, 324–332. [[CrossRef](#)]
25. Turton, R.; Shaeiwitz, J.A.; Bhattacharyya, D.; Whiting, W.B. *Analysis, Synthesis, and Design of Chemical Processes*, 5th ed.; Pearson: Upper Saddle River, NJ, USA, 2018.
26. Brown, T. *Engineering, Economics and Economic Design for Process Engineers*; CRC Press: Boca Raton, FL, USA, 2007.
27. Garrett, D.E. *Chemical Engineering Economics*; Van Nostrand Reinhold: New York, NY, USA, 1989.
28. Ministry of Industry. Orden ICT 778/2020, Bases Reguladoras de Concesión de Apoyo Financiero a la Inversión Industrial. 2020. Available online: <https://www.boe.es/boe/dias/2020/08/07/pdfs/BOE-A-2020-9399.pdf> (accessed on 7 September 2022).
29. Estadística Agraria Regional; Servicio de Asociacionismo Agrario y Estadísticas. *Precios En Origen*; Comunidad Autónoma de la Región de Murcia: Murcia, Spain, 2021.
30. ICIS Chemical Business. Available online: <http://www.icis.com/chemicals/channel-info-chemicals-a-z/> (accessed on 15 September 2022).
31. Okoro, O.V.; Nie, L.; Alimoradi, H.; Shavandi, A. Waste Apple Pomace Conversion to Acrylic Acid: Economic and Potential Environmental Impact Assessments. *Fermentation* **2022**, *8*, 21. [[CrossRef](#)]
32. Mancini, E.; Dickson, R.; Fabbri, S.; Udugama, I.A.; Ullah, H.I.; Vishwanath, S.; Gernaey, K.V.; Luo, J.; Pinelo, M.; Mansouri, S.S. Economic and Environmental Analysis of Bio-Succinic Acid Production: From Established Processes to a New Continuous Fermentation Approach with in-Situ Electrolytic Extraction. *Chem. Eng. Res. Des.* **2022**, *179*, 401–414. [[CrossRef](#)]
33. Short, W.; Packey, D.J.; Holt, T. *A Manual for the Economic Evaluation of Energy Efficiency and Renewable Energy Technologies*; National Renewable Energy Laboratory: Golden, CO, USA, 1995.

Disclaimer/Publisher’s Note: The statements, opinions and data contained in all publications are solely those of the individual author(s) and contributor(s) and not of MDPI and/or the editor(s). MDPI and/or the editor(s) disclaim responsibility for any injury to people or property resulting from any ideas, methods, instructions or products referred to in the content.